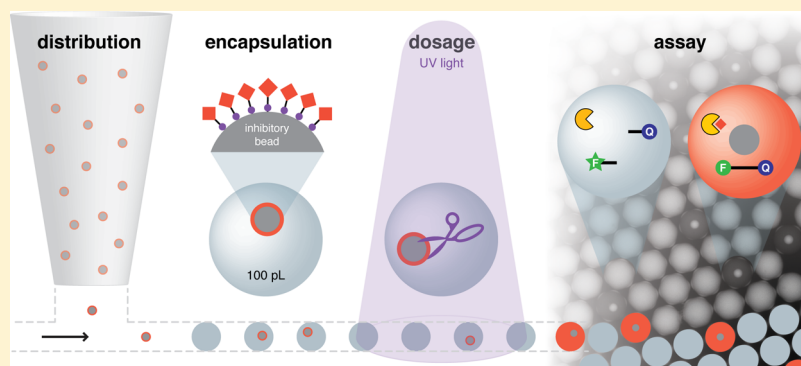# Microfluidic Bead Suspension Hopper

Alexander K. Price, Andrew B. MacConnell, and Brian M. Paegel*

Department of Chemistry, The Scripps Research Institute, Jupiter, Florida 33458, United States

**S** *Supporting Information*

**ABSTRACT:** Many high-throughput analytical platforms, from next-generation DNA sequencing to drug discovery, rely on beads as carriers of molecular diversity. Microfluidic systems are ideally suited to handle and analyze such bead libraries with high precision and at minute volume scales; however, the challenge of introducing bead suspensions into devices before they sediment usually confounds microfluidic handling and analysis. We developed a bead suspension hopper that exploits sedimentation to load beads into a microfluidic droplet generator. A suspension hopper continuously delivered synthesis resin beads (17 $\mu$m diameter, 112,000 over 2.67 h) functionalized with a photolabile linker and pepstatin A into picoliter-scale droplets of an HIV-1 protease activity assay to model ultraminiaturized compound screening. Likewise, trypsinogen template DNA-coated magnetic beads (2.8 $\mu$m diameter, 176,000 over 5.5 h) were loaded into droplets of an in vitro transcription/translation system to model a protein evolution experiment. The suspension hopper should effectively remove any barriers to using suspensions as sample inputs, paving the way for microfluidic automation to replace robotic library distribution.

High-throughput robotic chemistry and biology, the paradigm that drove the Human Genome Project[1] and the Molecular Libraries Initiative,[2] has reached a technology development plateau after decades of incremental improvements to existing microplate-based fluid-handling.[3] Where microplate miniaturization has not broken the microliter-scale, microfluidic water-in-oil droplets, the picoliter equivalents of microplate wells, effectively reduce reaction volumes by 5 orders of magnitude. However, performing assays such as PCR, enzyme kinetics, directed evolution, and drug screening[4−8] at the droplet scale introduces a common front-end engineering challenge: individual droplets must eventually house multiple copies of a distinct library member. Nucleic acid libraries can be stochastically diluted, compartmentalized, and then amplified in situ from single progenitor molecules (e.g., PCR, rolling circle amplification, cellular replication),[9,10] although this strategy is not applicable to other types of molecular libraries.

A general solution to interfacing both biological and chemical diversity with droplet-scale analysis lies in preparing and storing the diversity on solid phase resin beads. Beads are excellent delivery vehicles because each bead can harbor multiple copies (up to ∼1 pmol, depending on surface chemistry and bead size) of a unique library member. For example, emulsion PCR amplification generates bead-based gene libraries[11] while split-

and-pool combinatorial synthesis[12,13] efficiently yields bead-based small molecule libraries. Bead libraries (and microparticles in general), however, are challenging media for microfluidic analysis because device loading must be complete before the suspension has settled (e.g., in a syringe barrel, tubing, etc.). Larger, denser beads exacerbate this loading problem because they sediment even more quickly. Ironically, it is easier to make a bead in situ[14,15] than it is to load one. Here, we present a simple method for introducing large bead populations to microfluidic devices using a "suspension hopper" that exploits a suspension's tendency to sediment. Model ultraminiaturized compound screening and directed evolution applications, each employing a different resin particle, illustrate the general applicability of the suspension hopper to distribute multiple copies of a unique molecule into droplets.

## ■ EXPERIMENTAL SECTION

**Device Operation and Imaging.** Aqueous droplets (∼100 pL) in oil were generated at a flow focusing channel intersection.[16] The oil phase consisted of (50:46:4 w/w/w)

silicone oil (DMF-A-6CS, Shin-Etsu, Akron, OH), mineral oil, and surfactant (KF-6038, Shin-Etsu). Oil (0.9 $\mu$L/min) was driven into the circuit through the OIL inlet, and aqueous phase (PSS, 0.3 $\mu$L/min) was driven into the circuit through the BUF inlet. Droplet generation frequency was measured using an inverted epifluorescence microscope (10×, 0.25 NA, Axio Observer A1, Zeiss, Thornwood, NY) equipped with a high-speed CCD (500 fps, 640 × 480 res, NR4S1, Integrated Design Tools, Tallahassee, FL). After generation, the droplets enter a 200 $\mu$m-wide channel for dynamic imaging. The droplet stream was dispensed into PDMS wells prefilled with oil (~50 $\mu$L) for experiments requiring continuous fluorescence monitoring.

**Gravity-Based Bead Introduction and Dynamic Imaging.** The suspension hopper is a modified pipet tip (L-200, Rainin Instrument, Oakland, CA). The filter was excised from the tip, and a PDMS plug (4 mm diameter) was cemented into the larger end with uncured PDMS. Once filled with a bead suspension, the hopper was inserted into the LIB inlet downstream from BUF inlet. Image acquisition utilized an inverted fluorescence microscope (5×, 0.12 NA, AxioCam ICm1, Zeiss). As the beads settled into the circuit, 10 images were captured (1 Hz) every 10 min for up to 6 h (Figure S1, Supporting Information). Image data were analyzed (ImageJ, NIH, Bethesda MD) to tally droplets encapsulating 0 beads, 1 bead, 2 beads, etc.

**Photolytic Cleavage of Compound from Beads.** Droplets encapsulating beads displaying fluorescent peptide (Figure S2, synthesis and characterization details in Supporting Information) on their surface were dispensed into wells as described. Droplets were dosed with UV light from a X-Cite 120Q lamp (Lumen Dynamics Group Inc., Mississauga, Canada) through an open objective port using Zeiss filter set 49 ($\lambda_{ex}$ = 365 nm; $\lambda_{dc}$ = 395 nm; $\lambda_{em}$ = 445/50 nm). Exposure energy (2−860 J/cm$^2$) was measured using a photometer equipped with an I-line sensor (ILT 1400-A and XRL340B, International Light Technologies, Peabody, MA). Droplets were imaged (10×, 0.25 NA) in both bright field and fluorescence mode through Zeiss filter set 38HE ($\lambda_{ex}$ = 470/40 nm; $\lambda_{dc}$ = 495 nm; $\lambda_{em}$ = 525/50 nm). Image data were analyzed (ImageJ) to determine droplet size, bead size, and mean droplet fluorescence (Figure S3, Supporting Information).

**Droplet-Based HIV-1 Protease Assay.** The model droplet-based compound screen used a microfluidic circuit with two aqueous inputs that combine immediately prior to the droplet-generating intersection (Figure S4, Supporting Information). One aqueous input (0.3 $\mu$L/min) contained fluorogenic substrate (1.25×) and Alexa Fluor 647-dextran (2.67 $\mu$M) as an internal standard in assay buffer. The other aqueous input (0.2 $\mu$L/min) contained HIV-1 protease in vitro transcription/translation reaction product diluted 5-fold in assay buffer. The combined inputs were dispersed into droplets (~100 pL) by flow-focusing with oil (1.1 $\mu$L/min). A suspension hopper was loaded with a filtered (20 $\mu$m mesh, CellTrics, Partec GmbH, Görlitz, Germany) suspension of beads displaying pepstatin A (140 $\mu$L, 1 mg/mL, Figure S5, Supporting Information; synthesis and characterization details in Supporting Information) and inserted into the device. Droplets were dispensed into wells and dosed with UV light (0−99 J/cm$^2$) as described previously, liberating up to 600 fg of pepstatin A from each bead. After UV irradiation, the wells were incubated (2 h, 37 °C). Droplets were imaged as before

using the epifluorescence microscope and filter set 38HE for the probe and a custom filter set (Omega Optical, Inc., Brattleboro, VT) for the internal standard ($\lambda_{ex}$ = 600/50 nm; $\lambda_{dc}$ = 640 nm; $\lambda_{em}$ = 650 nm). Image data (Figure S6, Supporting Information) were analyzed (ImageJ) to measure mean droplet intensity.

**Droplet-Based in Vitro Expression of Trypsin.** Trypsin was expressed in droplets of in vitro transcription/translation (IVTT) reagent using the dual-input microfluidic circuit (Figure S4, Supporting Information). The first aqueous input (0.1 $\mu$L/min, IVTT solution A) and second aqueous input (0.1 $\mu$L/min, IVTT solution B, 80 ng/mL enterokinase, 2× disulfide bond enhancer, 50 $\mu$M fluorogenic thrombin substrate) combined 1:1 to deliver fully reconstituted protein expression reaction mixture for droplet generation in oil (0.8 $\mu$L/min). A suspension hopper was loaded with magnetic beads (140 $\mu$L, 1,360 beads/$\mu$L) displaying the gene encoding trypsinogen (the zymogen precursor of trypsin) and inserted into the device as described. Droplets were dispensed into wells and incubated (3 h, 37 °C). Droplets were imaged using the epifluorescence microscope and filter set 38HE.

## RESULTS AND DISCUSSION

**Suspension Hopper Design.** We devised a solution to the bead-loading problem that exploits the natural tendency of beads to settle. Beads sediment from a capped cartridge ("suspension hopper") into a continuously perfusing carrier stream. Integrating the suspension hopper with a droplet generator (Figure 1A) provides a robust and scalable method
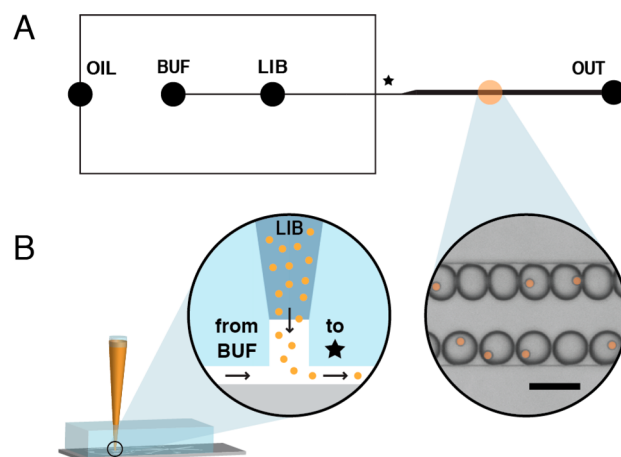


**Figure 1.** Suspension hopper circuit schematic and device operation. (A) Oil, buffer, and compound library beads enter at input ports OIL, BUF, and LIB. Buffer and beads combine with oil at the cross junction (★) to generate bead-containing droplets, which exit at the output port OUT. The micrograph (inset) shows beads (false orange color) distributed in picoliter droplets (scale = 100 $\mu$m). (B) The suspension hopper continuously introduces beads via sedimentation into LIB. Buffer flow orthogonal to sedimentation carries the beads to the cross junction for encapsulation.

for library bead distribution into picoliter-volume droplets. The suspension hopper funnels sedimenting beads into the LIB inlet port. As beads enter the device, buffer from the BUF inlet port sweeps the beads downstream (Figure 1B) to a cross-junction where two focusing oil streams encapsulate the beads in droplets. The hopper eliminates dead volume, and the cap prevents buffer from exiting the circuit at LIB.
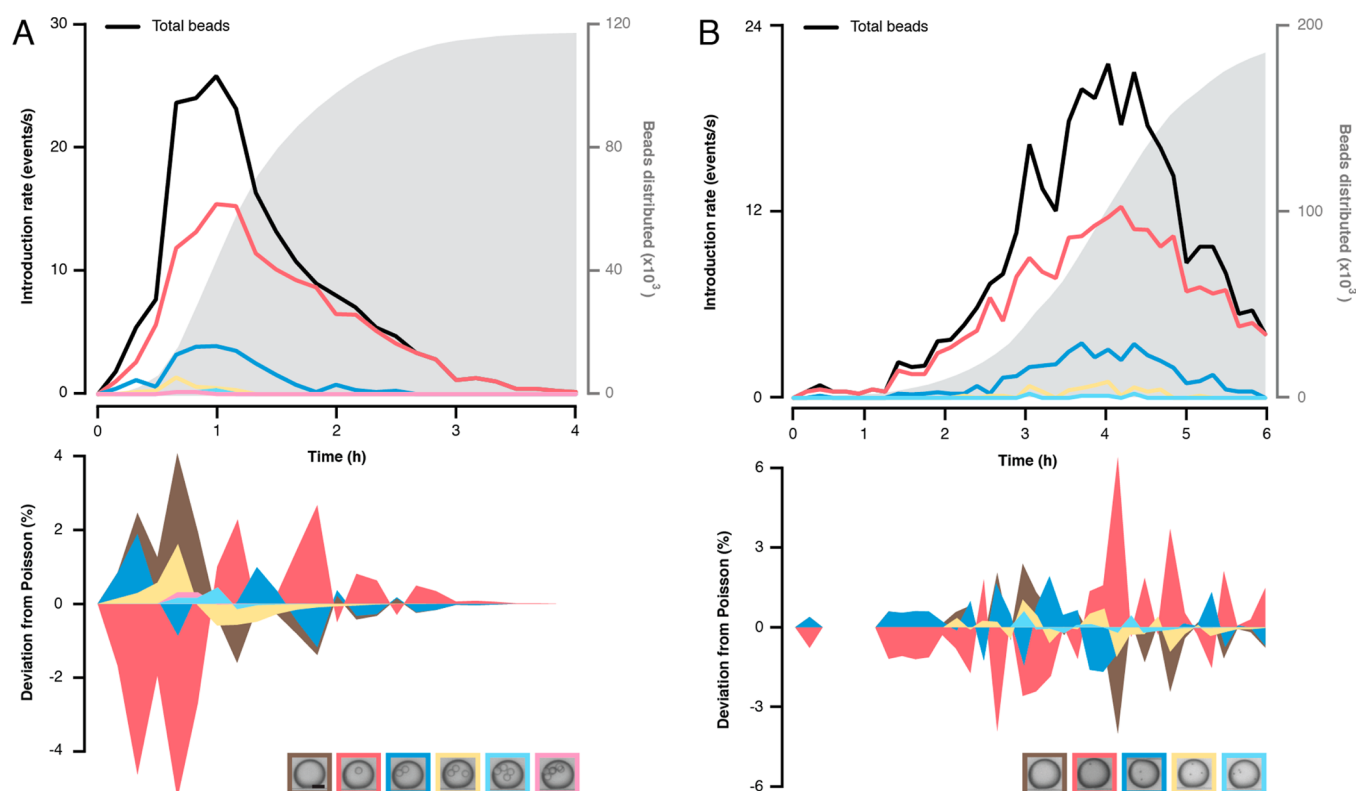
**Figure 2.** Statistical analysis of suspension hopper performance. Integration of the bead introduction rate (black trace, left axis) over time results in cumulative bead introduction for (A) 17 $\mu$m-diameter TentaGel synthesis resin and (B) 2.8 $\mu$m-diameter magnetic resin (gray, right axis). As beads are encapsulated into droplets (top color traces), the encounter probability deviates only slightly from the expected Poisson distribution (bottom color traces). 0, 1, 2, 3, 4, and 5 bead droplets are represented by brown, red, dark blue, yellow, light blue, and pink, respectively. Inset micrographs present example droplet classes. Scale = 30 $\mu$m.

The suspension hopper represents a significant departure from tedious bead delivery methods. For rapidly settling suspensions, introduction of high-density media such as glycerol can counteract sedimentation by modulating bead buoyancy. However, high-density additives can interfere with droplet generation and compromise biological activity. Constant agitation, an alternative, is difficult for suspensions housed in syringes and does not prevent bead sedimentation in connectors or tubing. More drastic measures such as suspending lab equipment vertically are impractical and potentially dangerous. Smaller beads can greatly reduce sedimentation rates, thus ameliorating problems with loading via syringe pumps; however, some applications require higher loading capacities (e.g., compound screening requires ~100 amol, 100 times the capacity of a 1 $\mu$m-diameter bead). The suspension hopper, engineered in response to these problems, introduces beads into a circuit continuously and reproducibly (Figure S7, Supporting Information). The simplicity of the design, inspired by the capped cell-perfusion chamber of Dishinger et al.[17] and the concept of gravity-driven flow,[18] should integrate easily with a wide variety of microfluidic circuits for analyzing microparticles.

**Bead Loading Performance.** We demonstrated the utility and scalability of the suspension hopper by distributing beads of two different sizes into droplets. A 140 $\mu$L hopper delivering a suspension of large-format Tentagel synthesis resin beads (~800,000 mL$^{-1}$, 17 $\mu$m diameter) continuously introduced 95% of the beads (112,000) within 2.67 h as shown in the integration of the bead introduction rate (Figure 2A, gray trace). A suspension hopper delivering small-format magnetic

beads (~1,360,000 mL$^{-1}$, 2.8 $\mu$m diameter) continuously introduced 95% of the beads (176,000) within 5.5 h (Figure 2B, gray trace). For both resin scales, bead introduction rate (Figure 2, black traces) exhibits a marked peak at 1 h for 17 $\mu$m-diameter resin and at 4 h for 2.8 $\mu$m-diameter resin. The rate of bead encapsulation into droplets (Figure 2, top colored traces) resulted in minor deviations between observed and expected bead encounter probabilities based on Poisson statistics (Figure 2, bottom colored traces). As bead introduction commences, there is a pronounced deficiency in the number of one-bead droplets and an accompanying surplus in multibead droplets and empty droplets. Toward the apex of bead introduction (0.8 h for Tentagel resin, 3.8 h for magnetic resin), this behavior inverts to a surplus of one-bead droplets and deviations from the Poisson distribution decay for all bead-droplet pairings.

The encounter probability of beads loaded from a suspension hopper and encapsulated in droplets agrees well with the Poisson distribution, indicating that it is a stochastic and therefore predictable process. Still, we observe slight but systematic deviations from the predicted probabilities. The surplus of multibead droplets prior to the bead introduction apex is likely due to the presence of bead clusters, which sediment more quickly in the hopper than single beads. The surplus of one-bead droplets after the bead introduction apex suggests systematic ordering independent of bead size. This effect may be similar to that of channel motifs designed to induce ordered particle flows and controlled encapsulation, leading to significant deviations from the expected Poisson distribution.[19,20] Even as the encounter probability changes

5041

dx.doi.org/10.1021/ac500693r | Anal. Chem. 2014, 86, 5039−5044

over the course of bead introduction, when 95% of each suspension has been encapsulated, 82.6% and 79.6% of occupied droplets contain a single 17 $\mu$m or 2.8 $\mu$m bead, respectively. While the presence of one bead inside a droplet is ideal, there is a balance between minimizing multibead droplets and maximizing the size of the library in the hopper. Implementing larger droplet generation rates drives down the frequency of multibead droplets, facilitating the use of larger bead concentrations (Figure S8, Supporting Information).

**Photochemical Droplet Dosing.** After encapsulation, the desired reaction between the bead-displayed library member and the assay mixture can proceed. Molecules can remain on-bead for many screening applications, but it is highly advantageous for some screens, particularly small molecule screens, to be performed "off-bead,"[21−23] requiring the liberation of molecule from the bead surface (Figure 3A). A fluorescent peptide attached to synthesis resin beads via an *o*-nitrobenzyl photolabile linker (**1**, Figure S2, Supporting Information) served as a model compound to demonstrate ultraviolet (UV) photochemical droplet dosing. A suspension hopper introduced **1**-functionalized beads into the microfluidic circuit for encapsulation in droplets, collection in oil-filled PDMS wells, and exposure to varying doses of UV light to induce linker photolysis. Only the beads fluoresce prior to exposure. UV irradiation liberates **1** from the bead surface (Figure 3B). The droplet concentration of **1** plateaus at 32 $\mu$M after exposure, and an abundance of fluorophore remains linked to the bead. The variance associated with compound liberation in droplets is 8−10% RSD, with deviation in coupled bead and droplet volume (8% RSD) and photolabile linker coupling efficiency. Compound release from a sample of 15 encapsulated beads exhibits biphasic kinetics with $k_{fast} = 35 \pm 1 \times 10^3$ J$^{-1}$ and $k_{slow} = 9 \pm 3 \times 10^2$ J$^{-1}$ (Figure 3C), in agreement with previously observed *o*-nitrobenzyl linker photolysis kinetics.[24]

**Model Compound and Directed Evolution Screens.** One example application where off-bead functional assay can provide an advantage is droplet-scale compound screening. Synthesis resin beads functionalized with an *o*-nitrobenzyl photolabile linker and ~100 fmol of aspartyl protease inhibitor pepstatin A (**2**, Figures 4 and S5, Supporting Information) served as the positive control. A dual-aqueous-input circuit and suspension hopper encapsulated positive control beads in droplets containing HIV-1 protease activity assay. Once a bead is encapsulated with assay components, UV irradiation doses the droplet volume with **2**. HIV-1 protease digests the fluorogenic substrate in empty droplets, yielding high signal at the substrate fluorescence wavelength relative to signal at the internal standard fluorescence wavelength (Figure 4A). Bead-occupied droplets exhibit UV-dose-dependent [**2**], which inhibits HIV-1 protease activity and results in low substrate fluorescence relative to the internal standard fluorescence. The Z-factor (Z′), a measure of assay quality,[25] for droplets dosed with 99 J/cm$^2$ UV light is 0.82 whereas undosed droplets containing positive control beads exhibit insignificant HIV-1 protease inhibition (Figure S9, Supporting Information).

A second example screening application is a model droplet-scale directed evolution experiment. A biotinylated trypsinogen gene is attached to streptavidin-functionalized magnetic beads. A dual-aqueous-input circuit and suspension hopper introduced beads functionalized with DNA encoding the trypsinogen gene and encapsulated the beads in droplets of IVTT reagent mixed with tryptic fluorogenic substrate (Figure 4B). Transcription of trypsinogen mRNA from bead-displayed template DNA,
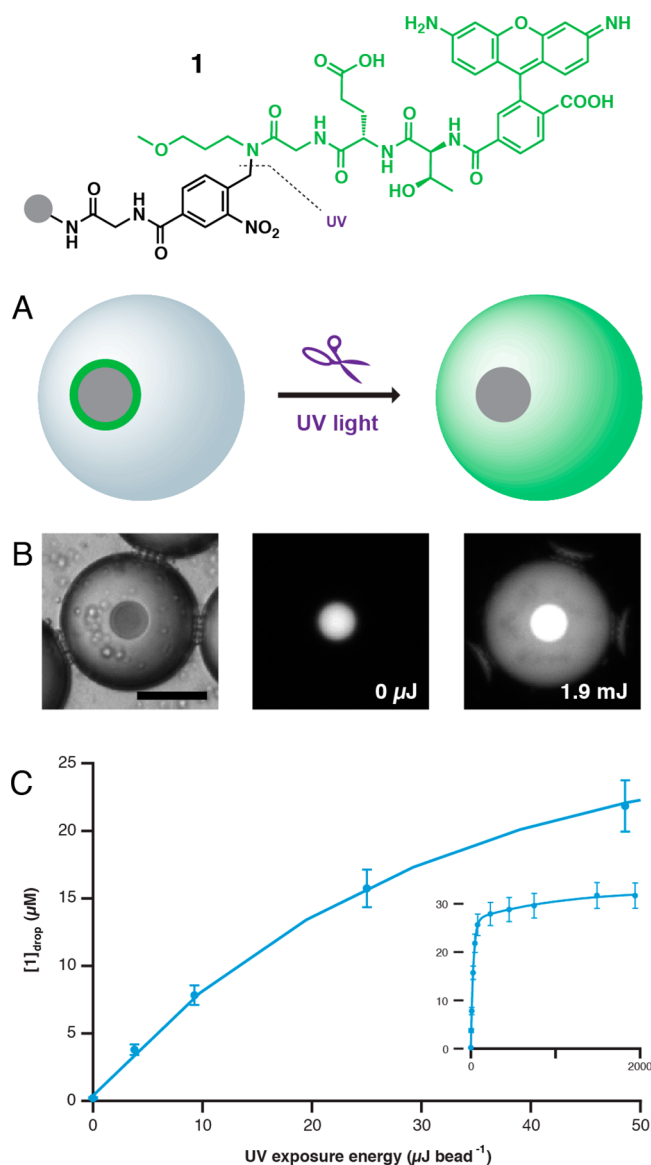


**Figure 3.** Photochemical compound dosing. TentaGel resin beads (gray circle) functionalized with an *o*-nitrobenzyl photolabile linker and rhodamine 110-labeled model compound (**1**, green) served as a reference for dosing studies. (A) Prior to UV exposure, **1** is localized to the bead. UV irradiation induces linker photolysis, liberating **1** from the surface and allowing it to diffuse throughout the droplet. (B) Droplets imaged in bright field (left, scale = 30 $\mu$m) and fluorescence mode before (middle) and after (right) UV exposure illustrate experimentally the liberation of **1** from the bead and concomitant droplet dosing. (C) Photolytic cleavage of **1** from the bead surface as a function of UV dose (*n* = 15 droplets) exhibits biphasic kinetics (cleavage kinetics for high UV doses, inset).

mRNA translation of the zymogen trypsinogen, and enterokinase-catalyzed cleavage of the synthetic propeptide from the zymogen N terminus yielded active trypsin. IVTT of template DNA and concomitant proteolytic digestion of quenched substrate to fluorescent product only occurred in bead-occupied droplets; empty droplets did not exhibit detectable tryptic activity. Although dilution of template to the single molecule limit is the simplest method for populating each droplet with a single library element, one molecule in a 100 pL droplet is insufficient template concentration for generating detectable tryptic activity. Template-functionalized beads,
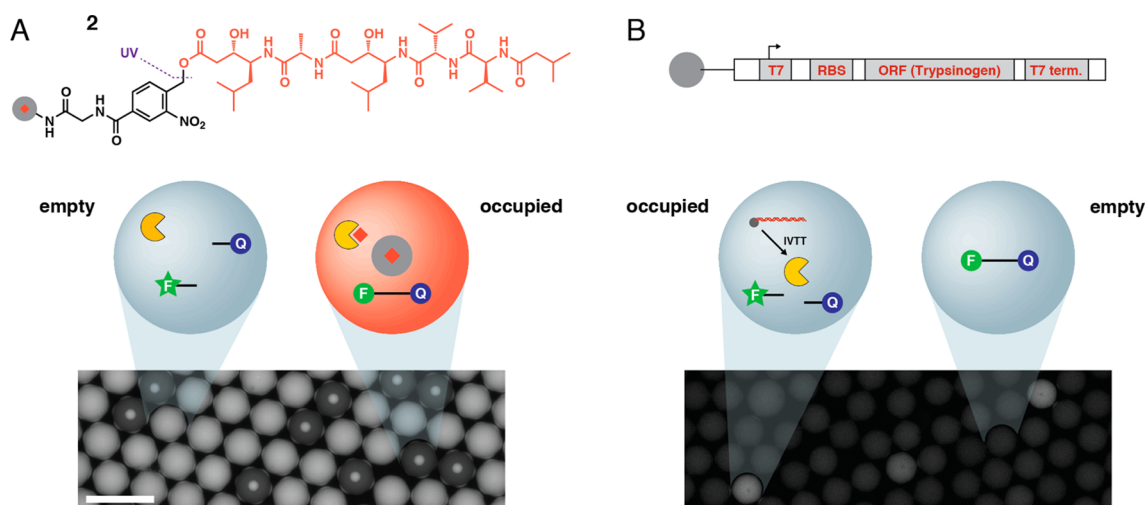
**Figure 4.** Bead-based assays in picoliter-scale droplets. (A) UV-photocleavable pepstatin A (**1**, red) attached to TentaGel resin beads (gray circle with red diamond) were distributed into droplets along with HIV-1 protease (yellow), fluorogenic HIV-1 protease substrate (F-Q), and internal standard. After UV exposure, bead-occupied droplets contain significant pepstatin A concentration (red droplet), inhibiting proteolytic F-Q digestion. In empty negative control droplets, F-Q proteolysis is uninhibited (blue droplet). (B) Magnetic beads functionalized with trypsinogen gene were distributed into droplets containing IVTT reagent, enterokinase, and a fluorogenic trypsin substrate (F-Q). In occupied droplets, trypsin expression leads to substrate proteolysis and fluorescence. No trypsin is expressed in empty droplets, and the substrate remains quenched. Scale = 100 μm.

however, enable efficient droplet-scale IVTT by delivering ~10,000 molecules to each droplet (~0.2 nM), which collectively yield robust proteolytic activity after 3 h.

Droplet-scale miniaturization is poised to revolutionize biological and chemical library screening. The ability to perform millions of reactions using only 100 μL of material trivializes the cost of screening reagents and opens up new avenues for assay development. For instance, we generated enough HIV-1 protease for millions of droplets from its gene in 2.5 h using ordinarily cost-prohibitive IVTT reagents. The amount of fluorogenic peptide probe sourced from either of two (thrombin or HIV-1 protease) commercial biochemical activity assay kits intended for ~100 microplate-scale reactions is sufficient for 15 droplet-scale screening campaigns, performing ~50 million total assay reactions. Assays that require all constituents to be free in solution can be performed with photochemical droplet dosing. A single 17 μm-diameter synthesis resin bead displays ~100 fmol sites available for functionalization, thus cleaving only 1% of sites will generate a 10 μM solution within a 100 pL droplet. This mode of droplet dosing does not require mechanical agitation of the droplet interface and is tunable over several orders of magnitude. Further system engineering is now required to integrate this process with bead loading and droplet generation to recapitulate the entire robotic compound distribution front end of an HTS facility in a single microfluidic circuit.

## CONCLUSIONS

Picoliter-scale droplet screening coupled with microfluidic integration can eventually obsolete robotic sample handling, but an efficient and scalable strategy for distributing discrete library elements into droplets remains a significant and unmet challenge.[26] Although diversity preparation in situ is possible by chemical synthesis[27] or amplification from single progenitors,[9] it is often advantageous to decouple library preparation from screening.[28] Particles are convenient to this end because they can serve both as synthesis scaffold and clonal polyvalent vehicles, ranging in size from viruses[29] and cells[30] to ~100 μm-

diameter beads.[31,32] Compared to biological scaffolds, beads can display a wider array of chemotypes (e.g., small molecules, peptides, dsDNA). Their large size translates to valency sufficient for dosing droplets with a range of cargo concentrations typical of screening-type experiments, but simultaneously raises problems associated with suspension settling in microfluidic circuitry. The suspension hopper is a simple and scalable front-end component that can interface large bead-based libraries with downstream integrated microfluidic automation. Populations of >100,000 beads were continuously introduced to a microfluidic circuit and distributed into droplets within hours. Encapsulation of the introduced beads is stochastic, allowing prediction of bead distribution via the Poisson distribution. Incorporation of a photocleavable linker allows tunable dosing of bead-occupied droplets with compound in applications that require off-bead screening. Taken together, the suspension hopper provides a critical bridge that connects bead-based molecular diversity to picoliter-scale analysis and will drive innovation toward a sustainable and distributed microfluidic bead library screening platform.

## ASSOCIATED CONTENT

**ⓢ Supporting Information**

Experimental details and additional results. This material is available free of charge via the Internet at http://pubs.acs.org.

## AUTHOR INFORMATION

**Corresponding Author**

*E-mail: briandna@scripps.edu.

**Notes**

The authors declare no competing financial interest.

## ACKNOWLEDGMENTS

## ■ REFERENCES

(1) Lander, E. S.; et al. *Nature* **2001**, *409*, 860−921.

(2) Austin, C. P.; You, A. J.; Brady, L. S.; Jackman, R. J.; Insel, T. R.; Whitesides, G. M.; Collins, F. S.; Schreiber, S. L. *Science* **2004**, *306*, 1138−1139.

(3) Hertzberg, R. P.; Pope, A. J. *Curr. Opin. Chem. Biol.* **2000**, *4*, 445−451.

(4) Huebner, A.; Olguin, L. F.; Bratton, D.; Whyte, G.; Huck, W. T. S.; de Mello, A. J.; Edel, J. B.; Abell, C.; Hollfelder, F. *Anal. Chem.* **2008**, *80*, 3890−3896.

(5) Baret, J.-C.; Miller, O. J.; Taly, V.; Ryckelynck, M.; El-Harrak, A.; Frenz, L.; Rick, C.; Samuels, M. L.; Hutchison, J. B.; Agresti, J. J.; Link, D. R.; Weitz, D. A.; Griffiths, A. D. *Lab Chip* **2009**, *9*, 1850−1858.

(6) Paegel, B. M.; Joyce, G. F. *Chem. Biol.* **2010**, *17*, 717−724.

(7) Sun, S.; Slaney, T. R.; Kennedy, R. T. *Anal. Chem.* **2012**, *84*, 5794−5800.

(8) Eastburn, D. J.; Sciambi, A.; Abate, A. R. *Anal. Chem.* **2013**, *85*, 8016−8021.

(9) Mazutis, L.; Araghi, A. F.; Miller, O. J.; Baret, J.-C.; Frenz, L.; Janoshazi, A.; Taly, V.; Miller, B. J.; Hutchison, J. B.; Link, D.; Griffiths, A. D.; Ryckelynck, M. *Anal. Chem.* **2009**, *81*, 4813−4821.

(10) Kiss, M. M.; Ortoleva-Donnelly, L.; Beer, N. R.; Warner, J.; Bailey, C. G.; Colston, B. W.; Rothberg, J. M.; Link, D. R.; Leamon, J. H. *Anal. Chem.* **2008**, *80*, 8975−8981.

(11) Dressman, D.; Yan, H.; Traverso, G.; Kinzler, K. W.; Vogelstein, B. *Proc. Natl. Acad. Sci. U.S.A.* **2003**, *100*, 8817−8822.

(12) Lam, K. S.; Salmon, S. E.; Hersh, E. M.; Hruby, V. J.; Kazmierski, W. M.; Knapp, R. J. *Nature* **1991**, *354*, 82−84.

(13) Furka, Á.; Sebestyen, F.; Asgedom, M.; Dibo, G. *Int. J. Pept. Protein Res.* **1991**, *37*, 487−493.

(14) Xu, S. Q.; Nie, Z. H.; Seo, M.; Lewis, P.; Kumacheva, E.; Stone, H. A.; Garstecki, P.; Weibel, D. B.; Gitlin, I.; Whitesides, G. M. *Angew. Chem., Int. Ed.* **2005**, *44*, 724−728.

(15) Chueh, B.-H.; Zheng, Y.; Torisawa, Y.-S.; Hsiao, A. Y.; Ge, C.; Hsiong, S.; Huebsch, N.; Franceschi, R.; Mooney, D. J.; Takayama, S. *Biomed. Microdevices* **2010**, *12*, 145−151.

(16) Anna, S. L.; Bontoux, N.; Stone, H. A. *Appl. Phys. Lett.* **2003**, *82*, 364.

(17) Dishinger, J. F.; Reid, K. R.; Kennedy, R. T. *Anal. Chem.* **2009**, *81*, 3119−3127.

(18) Huh, D.; Bahng, J. H.; Ling, Y.; Wei, H.-H.; Kripfgans, O. D.; Fowlkes, J. B.; Grotberg, J. B.; Takayama, S. *Anal. Chem.* **2007**, *79*, 1369−1376.

(19) Edd, J. F.; Di Carlo, D.; Humphry, K. J.; Köster, S.; Irimia, D.; Weitz, D. A.; Toner, M. *Lab Chip* **2008**, *8*, 1262−1264.

(20) Kemna, E. W. M.; Schoeman, R. M.; Wolbers, F.; Vermes, I.; Weitz, D. A.; van den Berg, A. *Lab Chip* **2012**, *12*, 2881−2887.

(21) Alluri, P. G.; Reddy, M. M.; Bachhawat-Sikder, K.; Olivos, H. J.; Kodadek, T. *J. Am. Chem. Soc.* **2003**, *125*, 13995−14004.

(22) Chen, X.; Tan, P. H.; Zhang, Y.; Pei, D. *J. Comb. Chem.* **2009**, *11*, 604−611.

(23) Liang, R.; Yan, L.; Loebach, J.; Ge, M.; Uozumi, Y.; Sekanina, K.; Horan, N.; Gildersleeve, J.; Thompson, C.; Smith, A.; Biswas, K.; Still, W. C.; Kahne, D. *Science* **1996**, *274*, 1520−1522.

(24) Il'ichev, Y. V.; Schwörer, M. A.; Wirz, J. *J. Am. Chem. Soc.* **2004**, *126*, 4581−4595.

(25) Zhang, J.; Chung, T.; Oldenburg, K. *J. Biomol. Screening* **1999**, *4*, 67−73.

(26) Brouzes, E.; Medkova, M.; Savenelli, N.; Marran, D.; Twardowski, M.; Hutchison, J. B.; Rothberg, J. M.; Link, D. R.; Perrimon, N.; Samuels, M. L. *Proc. Natl. Acad. Sci. U.S.A.* **2009**, *106*, 14195−14200.

(27) Theberge, A. B.; Mayot, E.; El-Harrak, A.; Kleinschmidt, F.; Huck, W. T. S.; Griffiths, A. D. *Lab Chip* **2012**, *12*, 1320−1326.

(28) Stapleton, J. A.; Swartz, J. R. *PLoS One* **2010**, *5*, No. e15275.

(29) Granieri, L.; Baret, J.-C.; Griffiths, A. D.; Merten, C. A. *Chem. Biol.* **2010**, *17*, 229−235.

(30) Agresti, J. J.; Antipov, E.; Abate, A. R.; Ahn, K.; Rowat, A. C.; Baret, J.-C.; Marquez, M.; Klibanov, A. M.; Griffiths, A. D.; Weitz, D. A. *Proc. Natl. Acad. Sci. U.S.A.* **2010**, *107*, 4004−4009.

(31) You, A. J.; Jackman, R. J.; Whitesides, G. M.; Schreiber, S. L. *Chem. Biol.* **1997**, *4*, 969−975.

(32) Upert, G.; Merten, C. A.; Wennemers, H. *Chem. Commun.* **2010**, *46*, 2209−2211.

5044

dx.doi.org/10.1021/ac500693r | *Anal. Chem.* 2014, 86, 5039−5044